Environmental Science and Pollution Research (2023) 30:12005–12019
https://doi.org/10.1007/s11356-022-22742-1

RESEARCH ARTICLE

Preferred injection method and curing mechanism analysis for the curing of loose Pisha sandstone based on microbially induced calcite precipitation

Zhuojun Feng[1] · Xiaoli Li[1] · Xinhang Shao[1] · Liming Wang[1]

Received: 19 May 2022 / Accepted: 22 August 2022 / Published online: 14 September 2022

Abstract

As a loose rock formation with low lithogenic property, low structural strength, and poor intersand cementation, Pisha sandstone is susceptible to chemical weathering and extreme soil erosion and has become an important source of sediment for the Yellow River. There is limited information available on the conditions of microbial distribution homogeneity under grain-mediated conditions in Pisha sandstones, as well as on the influence of dissolved minerals on calcium carbonate morphological mechanisms. In this paper, microbially induced calcium carbonate deposition was used to reinforce and improve the loose Pisha sandstone. First, the influence laws of the single-phase/self-absorption two-phase injection method and added solvent on the curing indexes such as curing volume, curing depth, calcium carbonate yield, and unconfined compressive strength of the specimens were discussed. Field emission scanning electron microscopy, Fourier transform infrared spectroscopy, and X-ray diffraction spectroscopy were used to analyze the microstructure of the cemented sand columns, as well as the mineral phases and distribution of the biomineralization products mechanistically. The results demonstrated that the single-phase injection treatment could only achieve local solidification of the Pisha sandstone sand column, whereas the self-absorption two-phase injection method could result in a more uniform spatial distribution of bacteria and a monolithic specimen, in which the calcium carbonate yield increased with increasing low concentration $CaCl_2$ injection. The compressive strength appeared to increase significantly, and the effect of the applied liquid $CO(NH_2)_2$ was not obvious. Montmorillonite underwent dissolution during the mineralization process, eliminating the characteristics of Pisha sandstone swelling in water. Under the effect of biomineralization, calcium carbonate crystals are formed to wrap around the Pisha sandstone particles, changing their particle size and increasing the interparticle roughness. Meanwhile, the interstices between particles are filled via calcium carbonate precipitation, effectively forming cementation points that can significantly improve the strength of the Pisha sandstone. The results of this study provide a theoretical basis for the application of biomineralization technology in the ecological restoration of Pisha sandstone areas.

Keywords Microbial mineralization · Microbial grouting · Pisha sandstone · Mechanical properties · Soil improvement · Microstructure

Responsible Editor: Philippe Garrigues

✉ Xiaoli Li
sjylxl@imau.edu.cn

Zhuojun Feng
shinefzj@yeah.net

Xinhang Shao
1311383074@qq.com

Liming Wang
1164761443@qq.com

[1] College of Water Resources and Civil Engineering, Inner Mongolia Agricultural University, Hohhot 010018, People's Republic of China

Introduction

Pisha sandstone is widely distributed in the Yellow River basin and the adjacent areas of the Ordos Plateau near Shanxi, Shaanxi, and Inner Mongolia (Yao et al. 2019). It is mainly composed of minerals such as quartz, montmorillonite, feldspar, and calcite, of which the feldspar weathering material is kaolinite, which has poor impact resistance. The cementing material is mainly calcite and dolomite; however, the cementing force can be weakened by reaction with water. The clay material is montmorillonite, which expands in volume when it comes into contact with water (Liang

et al. 2019). Moreover, many scholars have kept up in-depth research on the natural mineral structure of the Pisha sandstone and surface exfoliation under natural conditions (Zhang et al. 2019a, b; Zhang et al. 2019a, b).

In recent years, basic research work on Pisha sandstone has gradually shifted to environmental management and applications (Wang et al. 2020; Yang et al. 2019; Cheng et al. 2016a, b). Traditional methods of soil consolidation mainly include mechanical compaction and chemical–physical composite reinforcement. The engineering properties of Pisha sandstone can be improved when mixed with cement (Liu et al. 2020; Geng and Li. 2022), and microscopic analysis revealed that the Pisha sandstone cement soil has better erosion resistance (Geng et al. 2022). Cement is commonly used as an inorganic curing agent for soil improvement; however, the production of one ton of cement clinker emits 0.9 tons of CO_2, as well as other air pollutants (Gong 2022). To reduce the amount of cement used, many scholars have prepared geopolymer-Pisha sandstone hydroclay using alkali-excited minerals with a volcanic ash effect (e.g., fly ash and metakaolin), and studies have shown that the improved Pisha sandstone cement composite soil can meet the use of road base materials (Yang et al. 2021a; Li et al. 2021a, b; Zhao et al. 2021; Zhu and Li 2022). However, except for Na_2SiO_3, all other commonly used chemical building materials have a certain degree of toxicity (Zhao 2014). For example, most chemical grouting materials are highly alkaline and biotoxic, and they prevent vegetation from growing after curing. Additionally, their use is constrained by excessive environmental pollution. Hence, it is significant to study new gel materials that are energy efficient, pollute less, and have excellent performance.

Microbially induced calcite precipitation (MICP) is a new green building material technology that can effectively improve the disadvantages brought about by the traditional use of chemical building materials for soil reinforcement. Compared with traditional methods, it has the advantages of a simple mechanism, good fluidity, adjustable reaction rate, and cementation strength. The injection of a bacterial solution into loose sand particles, through the decomposition of urea by urease in microorganisms, produces carbonate ions, which combine with calcium ions in the solution to form a bonding and insoluble carbonate gel that binds loose particles together. It is used to improve the mechanical properties of sand and soil such as strength, stiffness, and resistance to liquefaction (Whiffin 2004). Presently, MICP technology is widely used in cementitious materials crack repair (Qian et al. 2021a, b), coastal slope protection, and foundation reinforcement (Cheng et al. 2013).

In microbially cured sandy soil tests, numerous factors influence the curing effect, including urease activity (Yang et al. 2021a, b), cement concentration (Li et al. 2021a, b), and grouting process (Hoang et al. 2018). After saturating the sand column with tap water flushing and grouting it with a two-stage injection method, it was discovered that the flushing was not conducive to bacterial immobilization on the surface of soil particles, and the efficiency of chemical conversion of calcium carbonate was reduced to less than 5% (Cheng et al. 2016a, b). When treating samples through different concentrations of cementing solutions, the use of highly concentrated solutions resulted in larger precipitation crystals that formed local blockages, resulting in uneven cementation, thus affecting the strength of microbially cured soils (Qabany and Soga 2013). Curing the specimens with pure/mixed bacterial solution injection revealed a more uniform distribution of calcium carbonate crystals within each region along the height direction of the specimens, as well as a dense filling of pores between loose sand particles (Cui et al. 2017). Furthermore, the grouting speed and amount of bacterial solution injection can affect the curing effect, with 1.0 and 1.2 times the pore volume of the sand body being the optimal amount of bacterial solution injection, and a grouting speed of 8 mL/min effectively improving the uniformity of silica sand reinforcement (Tian et al. 2021). While using the two-phase injection method to reinforce the sand column, the compressive strength of the part of the sand column near the injection point is lower than the other end (Rowshanbakht et al. 2016). The sand column was injected two to six times, and as the number of injections increased, the sand column's compressive strength and density also increased (Yu et al. 2018).

Presently, the microbial curing sandy soil technology has yielded promising results, based on the application of MICP technology in sandy soil curing in the field of construction engineering, to explore the application research of MICP technology in soil erosion of weathered loose Pisha sandstone in the Ordos. The mineral structure of montmorillonite in Pisha sandstones is distinctive, giving it adsorption, swelling, ion exchange, and cementation properties. It is subject to erosion when exposed to water. However, there is little research related to the effect of the mineral composition of the eroded mineral on calcium carbonate formation. In this paper, an experimental study of microbially induced calcium carbonate deposition for curing Pisha sandstone was conducted to compare the effects of the single-phase injection method, self-absorption biphasic injection method, and added solvent on the curing effect; analyze the variation in calcium carbonate yield, curing volume, curing depth, and unconfined compressive strength (UCS); and select the optimal curing improvement solution. The nucleation, crystal growth, and cementation mechanisms of biomineralization were analyzed using scanning electron microscopy (SEM) and X-ray diffraction (XRD), and the interactions between calcium mineralization products and Pisha sandstone particles were analyzed via Fourier transform infrared (FTIR)

spectroscopy. This research provides a theoretical basis for the microbial solidification of Pisha sandstone technology.

Test materials and test methods

Proportioning of bacterial solution and calcium source solution

The strain used in the Pisha sandstone curing test was *Sporosarcina pasteurii*, strain number CGMCC 1.3687, procured from the China General Microbial Strain Conservation and Management Center, and the main components and content of the medium were peptone 10 g/L, beef extract 5 g/L, urea 20 g/L, and sodium chloride 5 g/L. The solvent was distilled water, adjusted $pH = 7.3$. The mother liquor was inoculated into the sterilized fresh medium at the ratio of $V{:}V = 1{:}100$, inserted into the shaker at 30 ℃, 170 r/min, and incubated continuously for 24 h. The concentration of the bacterial solution was diluted to $OD = 0.6$ for use before the experiment. The calcium source solution used in this experiment consisted of 1 mol anhydrous calcium chloride (110.98 g/L) and 1 mol urea (60.06 g/L).

Test soil

Red Pisha sandstone (RPS) was taken from the Ordos region of Inner Mongolia, and the grain size composition and grain size gradation of the soil samples are shown in Fig. 1. The coefficient of inhomogeneity C_u was 3.1, and the coefficient of curvature C_c was 0.9. The test soil was classified as poorly graded sandy soil according to the Unified Soil Classification System. Figure 2 shows the results of the XRD analysis. The main mineral composition of RPS is quartz and feldspar, and the clay minerals are mainly montmorillonite and illite.

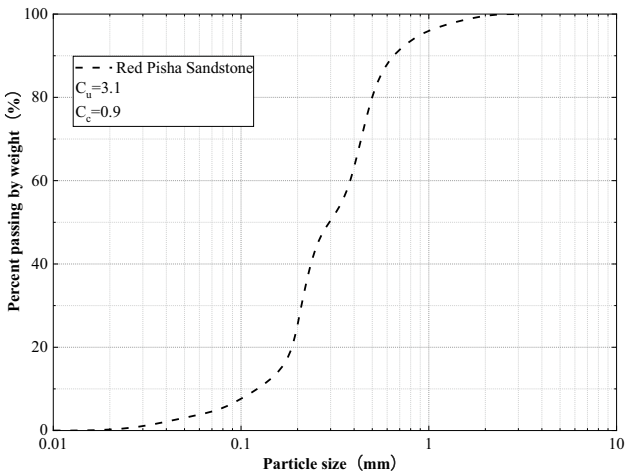

Fig. 1 The analysis of red Pisha sandstone particles

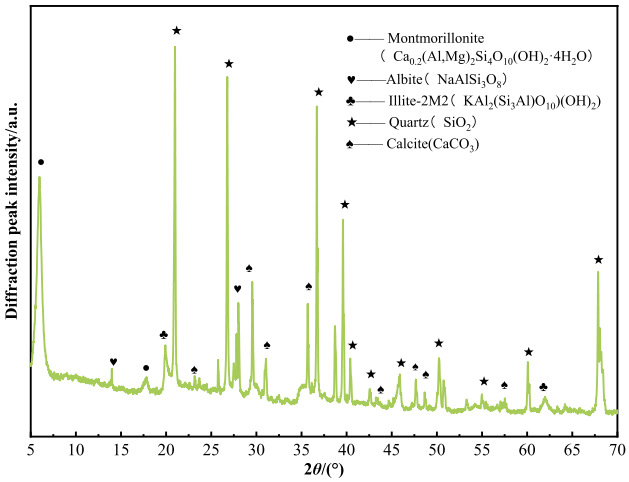

Fig. 2 XRD pattern of red Pisha sandstone particles

Pisha sandstone curing trial mold device

According to the geotechnical test methods standard (GB/T 50,123–2019), the Pisha sandstone curing specimen was made of a transparent Plexiglas tube with an inner diameter of 39 mm and a height of 80 mm (comprising two cylinders broken in half along the diameter to reduce specimen disturbance when taking the sample out of the mold), and the bottom of the curing device was a removable water filter mat cover, which was covered with small holes with an inner diameter of 2 mm to facilitate the natural slurry infiltration out of the device. Prior to the test, the test mold was sealed with transparent tape to prevent leakage, and the top and bottom surfaces of the device are padded with a nonwoven cotton cloth to prevent impact damage and loss of loose Pisha sandstone at the bottom during grouting. Figure 3 shows the schematic diagram of the microbial curing Pisha sandstone forming device.

Specimen preparation and test protocol

According to the geotechnical test method standard (GB/T 50,123–2019) relative density test method, the natural dry density of Pisha sandstone was measured to be 1.125–1.421 g/cm^3. In this test, the dry density of the test soil was 1.31 g/cm^3, the volume of the test mold was 95 cm^3, and the Pisha sandstone particles with a mass of 125 g were weighed and added to the test mold. In this paper, the feasibility of microbial curing of Pisha sandstone was investigated using two casting methods: single-phase injection and self-absorption two-phase injection. The methods were used to optimize the curing effect by injecting a certain amount of $CaCl_2$ and $CO(NH_{2)2}$ solutions, as well as to investigate the effects of the MICP casting method and additional solvent on the characteristics of microbial curing of Pisha sandstone,

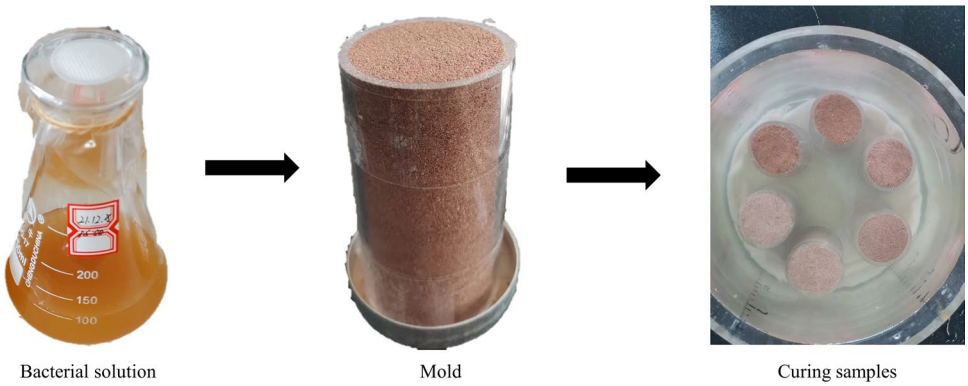

Fig. 3 Pisha sandstone biomineralization test device

Table 1 Experimental scheme for microbial curing of Pisha sandstone by single-phase injection method

Number	Type and dosage of the injected liquid	Number of cycles
T60	60 ml of bacterial solution	1
TC213	20 ml of bacterial solution, 10 ml $CaCl_2$	3
TC223	20 ml of bacterial solution, 20 ml $CaCl_2$	3
TU213	20 ml of bacterial solution, 10 ml of $CO(NH_2)_2$	3
TU223	20 ml of bacterial solution, 20 ml of $CO(NH_2)_2$	3

by measuring the calcium carbonate yield, curing volume, curing depth, and UCS of the cured specimens, combined with XRD, SEM, and FTIR analysis.

Curing treatment by single-phase injection method

Set up pure bacterium solution pouring control group T60, 60 mL of bacterium solution was injected continuously from the top, and the amount of injected bacterium solution was approximately 2 times the pore volume of Pisha sandstone. The pouring method of the extra liquid test group was as follows: (1) From the top, 20 mL of bacterial solution was injected. (2) After the injection of a bacterial solution, 10 or 20 mL of additional solvent (0.05 mol/L $CaCl_2$ and 1 mol/L $CO(NH_2)_2$) was added. Methods 1 and 2 were repeated and cycled three times more, with the flow rate controlled during the injection. Table 1 shows the test protocol.

After grouting, the specimens were left to stand for 8 h to allow the bacteria to fully adsorb on the pisiform-sandstone particles; after standing, the specimens were placed in a reaction vessel with a calcium source solution for maintenance. On the first day of maintenance, the top of the specimen was 1 cm away from the surface of the cementing solution to prevent the top of the specimen from being submerged at the beginning of the reaction, resulting in calcium carbonate flocculation blockage and to avoid the phenomenon of hollowing or swelling and cracking at the top due to the gas inside the specimen not being removed smoothly. Additionally, an air pump was used to connect the bubble stone to provide oxygen for bacterial growth and reproduction during the maintenance period. At the end of the first day of curing, the specimens were completely submerged and immersed for 6 days, to keep the liquid level of the cement always 2 cm above the top surface of the specimens.

Self-absorption two-phase injection method of curing treatment

Through pre-experiments, it was discovered that a dry Pisha sandstone particle, with a mass of 125 g could inhale a maximum of 40 mL of liquid. Therefore, the self-absorption two-phase injection method is as follows: (1) bottom treatment—place the test device in a Petri dish, inject 40 mL of bacterial solution into the Petri dish, make it naturally seep into the Pisha sand column, and leave it for 3 h so that the bacteria are fully adsorbed on the Pisha sandstone particles; (2) top treatment—after the bottom treatment is finished, inject 20 mL of bacterial suspension from the top. After the bacterial solution injection is finished, inject 10 or 20 mL of additional solvent (0.05 mol/L $CaCl_2$ and 1 mol/L $CO(NH_2)_2$); (3) filtrate treatment—once the filtrate leaked out from the bottom of the Petri dish, it was collected and mixed thoroughly before being injected from the top again and then left to stand for 5 h after the injection was completed, as shown in Table 2. Additionally, to compare the effect of the added solvent, a pure bacterial solution control B4T2 was set up.

Parameter testing of MICP-reinforced Pisha sandstone

Since the Pisha sandstone contains acid-soluble minerals, the determination of newly generated calcium carbonate could not be performed using the acid washing method, and the amount of calcium carbonate generated was quantified based on the change in mass before and after treatment of the cured specimens. After 7 days of reaction, the specimens were removed and washed with deionized water to remove

Table 2 Experimental scheme for microbial curing of Pisha sandstone by self-adsorption two-phase injection

Number	Type and dosage of the injected liquid	
	Upper injection port	Bottom injection port
B4T2	20 ml of bacterial solution	40 ml of bacterial solution
B4TC21	20 ml of bacterial solution, 10 ml $CaCl_2$	40 ml of bacterial solution
B4TC22	20 ml of bacterial solution, 20 ml $CaCl_2$	40 ml of bacterial solution
B4TU21	20 ml of bacterial solution, 10 ml of $CO(NH_2)_2$	40 ml of bacterial solution
B4TU22	20 ml of bacterial solution, 20 ml of $CO(NH_2)_2$	40 ml of bacterial solution

the residual caking solution. The specimens were then dried in a blast dryer at 60 ℃ until the mass was constant and the mass was measured. Due to the inhomogeneity of the cured specimens, the curing along the wall of the test mold is better than the curing along the middle part, and the minimum depth value of uncured at the side wall of the sand column is considered the minimum curing depth. Furthermore, the maximum curing depth value along the side wall of the sand column is considered the maximum curing depth, and the minimum curing depth to the maximum curing depth of this interval is considered the curing depth change interval.

A universal testing machine of WDW-100 M-type equipment company was used to test the lateral limitless compressive strength of the specimens after microbial curing and maintenance, with a loading rate of 1.0 mm/min until the specimens were destroyed. The damaged samples (pure bacterial solution control group, optimal curing group mixed with additional solvent) were thoroughly ground, tested for crystal composition using a multifunctional horizontal X-ray diffractometer of the RIKEN Ultima IV combination type, and analyzed for diffraction peak intensity, material composition, and crystalline surface constants. The functional groups in the specimens were detected via FTIR spectroscopy using Spectrum Two (PE, USA). To analyze the surface morphology of the Pisha sandstone amended soils, larger specimens were collected after destruction for cutting and processing, dried after alcohol, and coated with a thin layer of gold to improve the electrical conductivity. The microscopic morphology and structure were observed at magnifications, ranging from 500 to 10,000×, using a field emission scanning electron microscope with the FEI Quanta 250 FEG, USA.

Results

Effects of single-phase injection on macroscopic properties

The clear morphology of microbially cured Pisha sandstone is shown in Fig. 4, and the specimens treated with single-phase injection all showed the curing characteristics of better curing on one side of the sidewall. Particularly, the pure bacterial solution test group T60 showed an obvious hollow phenomenon, and when 10 mL of additional solvent was added for optimization, the specimens no longer showed a hollow phenomenon; thus, the integrity was enhanced. Additionally, the $CaCl_2$ treatment was more uniform compared with the $CO(NH_2)_2$ treatment. When 20 mL of additional solvent was added for optimization, the $CaCl_2$ treatment lowered the curing volume of the specimens, whereas the curing effect of the reinforced unilateral sidewall of the specimens after the $CO(NH_2)_2$ treatment. The curing effect was more significant.

As shown in Fig. 5, the calcium carbonate yields of TC213, TC223, and TU223 decreased by 33.06%, 55.52%, and 20.62%, respectively, compared with the pure bacterial solution injection specimen T60, whereas TU213 increased by 3.15%. The calcium carbonate yield significantly decreased when the additional solvent injection volume was 20 mL, demonstrating how the injection of the additive solution affected the chemical conversion efficiency of calcium carbonate.

When comparing the curing effects of T60, TC213, and TC223, it was observed that with an increase of 0.05 mol/L $CaCl_2$ injection, the curing volume of MICP-cured Pisha sandstone gradually decreased, the minimum curing depth first increased and then decreased, and the curing depth variation interval and the maximum curing depth first decreased and then increased. Compared with the T60 injected with a pure bacterial solution, the specimens injected with a calcium source were cured more uniformly, with a smaller curing depth variation interval and an average curing depth of 4 cm. Thus, the cementation effect was relatively good. When $CO(NH_2)_2$ solution was substituted for $CaCl_2$, that is, for the TU213 and TU223 groups, the MICP curing volume increased and the average curing depth was around 5 cm, which was slightly better than the calcium source. However, the curing depth variation interval increased and the overall curing uniformity decreased. From the curing depth results, the single-phase injection method for calcium carbonate deposition mostly operates in the middle and upper layers, and the cementation effect gradually declines along the depth direction, with no particle cementation at the bottom, which is scattered. The depth variation interval for the pure bacterial solution and urea injection is wider;

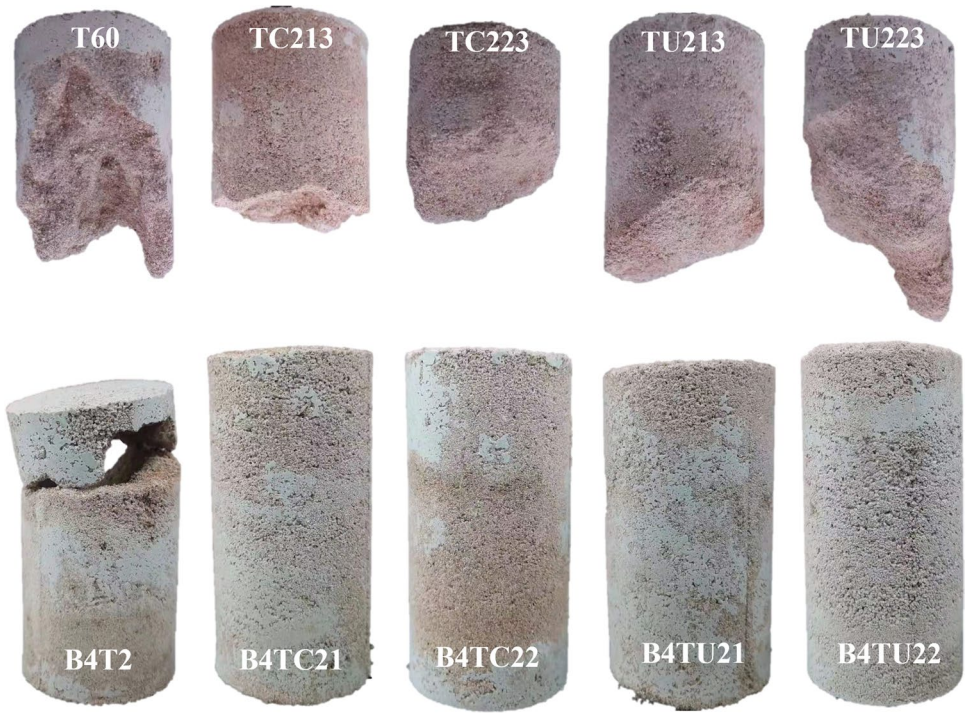

Fig. 4 Physiognomy of microbially cured Pisha sandstone

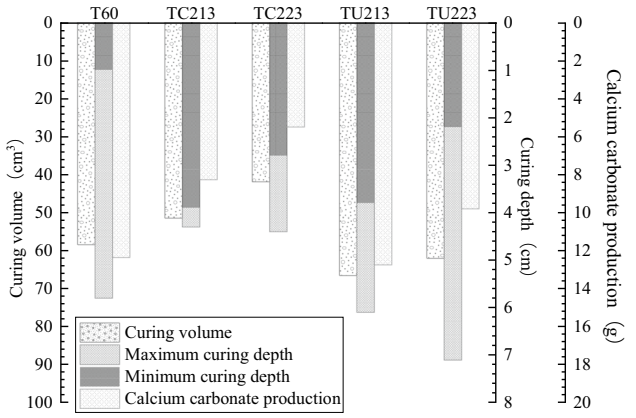

Fig. 5 The effect of single-phase injection method on curing volume, curing depth, and calcium carbonate yield

calcium source injection can increase the regularity of the distribution of bacterial solution, making curing more uniform along the depth direction, although there is noticeable local curing. Hoang et al. (2018) suggested that the calcium carbonate precipitate generated using the stepwise injection method was more uniform along the depth direction, which is slightly different from the results of this experiment.

This is probably attributed to the volume expansion of montmorillonite in the Pisha sandstone via water absorption, which reduces the pore volume inside the Pisha sandstone body, the decrease in internal channel pore size, and the decrease in the percolation capacity. Additionally, the agglomerates in the Pisha sandstone are easily dispersed and broken by fluid action. Fine mineral particles fall off, break and migrate from the large particles, and move in the pore channels with the fluid runoff, causing the pore channels to seal and become less connected. Simultaneously, the surface of the microbial cells with a negative charge, under the action of electrostatic force and closely arranged microbial cells repel each other. The introduction of $CaCl_2$ causes surface-negative ions and Ca^{2+} mutual adsorption, resulting in a charge-neutral amorphous calcium carbonate, which causes the bacterium's size to increase. Because the amorphous calcium carbonate has a certain bonding effect, migration occurs under the action of percolation, adsorption in the pore channel, or blocking of the pore channel, resulting in the bacterium staying in the upper half layer. When the $CaCl_2$ injection amount increased, more Ca^{2+} was introduced to further increase the size of the bacteria and intensify the retention effect of bacteria in the pore channel. This also explains the deteriorating effect of calcium source injection on the curing depth.

After replacing $CaCl_2$ with $CO(NH_{2)2}$ solution, bacteria migrated and adsorbed on the surface of Pisha sandstone particles at depth under the action of seepage. However, due to the expansion of montmorillonite to seal the pore channel, calcium carbonate was mainly concentrated at 2–4 cm of solidification depth. When $CO(NH_2)_2$ injection increased, the bacteria unattached to the Pisha sandstone particles were flushed out, the sand column solidification rate decreased, and the calcium carbonate production decreased. Simultaneously, the injection of the additional solvent caused the bacterial solution to flow along the side walls of the test mold,

thus reducing the amount of calcium carbonate production and conversion efficiency.

Effect of self-absorption two-phase injection on macroscopic properties

As seen in Fig. 4, in the self-absorption biphasic injection of the pure bacterial solution test group, the bottom curing effect is better than the top curing effect, whereas the sand column curing is unaffected after injecting the additional solvent treatment. This indicates that the bacteria will adhere to the bottom particles of the sand column of Pisha sandstone after the natural infiltration of the bacterial solution from the bottom. However, after the bottom treatment, the permeability of the sand column decreases, so the migration of bacteria will be slowed down when injecting the bacterial solution from the top. Additionally, when the additional solvent is injected and the filtrate is repeatedly poured, the migration time of bacteria can be prolonged, allowing them to adsorb on the deep Pisha sandstone particles and make the spatial distribution of bacteria more uniform. Furthermore, Pisha sandstone itself has adsorption properties, and the components of the culture medium in the bacterial solution are retained in the specimen during injection, providing nutrients for bacterial growth and reproduction.

In comparison with the calcium carbonate production of the B4T2 (14.118 g) pure bacterial solution control group, the calcium carbonate production of the two-way grouting test groups B4TC21, B4TC22, B4TU21, and B4TU22 increased by 33.96%, 54.99%, 40.40%, and 42.97%, respectively, as the applied slurry increased, as shown in Fig. 6. When the injection amount was 10 mL, the calcium source group produced less calcium carbonate than the urea group; when the injection amount was 20 mL, the calcium source group produced more calcium carbonate than the urea group, indicating that the low concentration of calcium source injection contributed to the increase in calcium carbonate production. Alternatively, the increase in urea injection amount had no obvious effect on calcium carbonate production, which was the result of the urease in bacteria decomposing urea to obtain energy to produce CO_3^{2-}. Nevertheless, in this process, the total system urease was not affected. The activity of the system urease will be reduced, as will the formation of calcium carbonate precipitation after contacting Ca^{2+}, which seals the pores in the sand column, decreasing the internal oxygen content of the sand column and an extremely rapid decrease in bacterial survival, which is not conducive to the generation of subsequent biomineralization products.

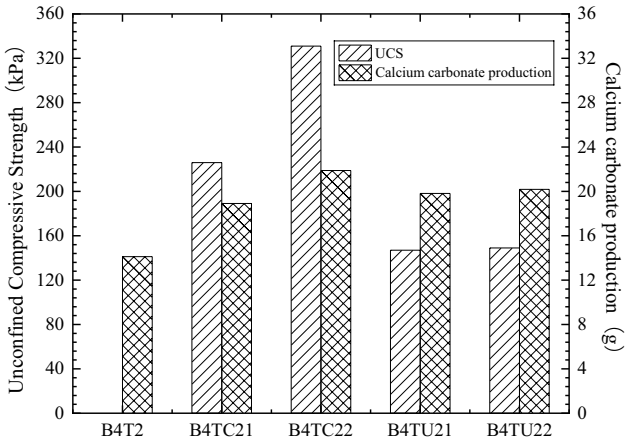

Fig. 6 The effect of self-adsorption biphasic injection on the yield of UCS and calcium carbonate

For the calcium source treatment groups B4TC21 and B4TC22, the calcium carbonate yield increased with the increase of the additional solvent injection from 10 to 20 mL, and the compressive strength increased with the increase of $CaCO_3$ yield, indicating that the formed calcium carbonate had the effect of cementing particles. Furthermore, for the urea treatment groups B4TU21 and B4TU22, the calcium carbonate yield was higher than that of B4TC21, but the compressive strength did not increase, indicating that the formed calcium carbonate had the effect of cementing particles. This indicates that the formed calcium carbonate precipitation cementation is poor.

Physical phase mechanism analysis based on XRD mapping

Due to the different properties and stabilities of different crystalline forms of calcium carbonate, there are several types of calcium carbonate crystals, which are primarily composed of six different phases, namely, calcite, sphalerite, aragonite, amorphous calcium carbonate, calcium carbonate hexahydrate, and calcium carbonate monohydrate (Yin et al. 2019; Atashgahi et al. 2020). Therefore, it is critical to determine the crystalline form of the generated calcium carbonate and its physical properties. The fragments of the cured sand column were selected, ground, and analyzed by the XRD, and the results are shown in Fig. 7.

Comparison of the microbial solidification test groups with the RPS and self-absorption two-phase injection revealed a significant change in the peak intensity of the diffraction peak corresponding to calcium carbonate at the (104) crystal plane. This indicates that the mineralization product formed by microbial induction is mainly calcite. Among them, the pure bacterial solution test group B4T2 displayed a strong sharp diffraction peak of the silica–aluminate phase after the microbial mineralization treatment. When the calcium source treatment groups B4TC21 and B4TC22 are compared, it can be seen that the intensity of the quartz diffraction peak corresponding to the (100) (112)

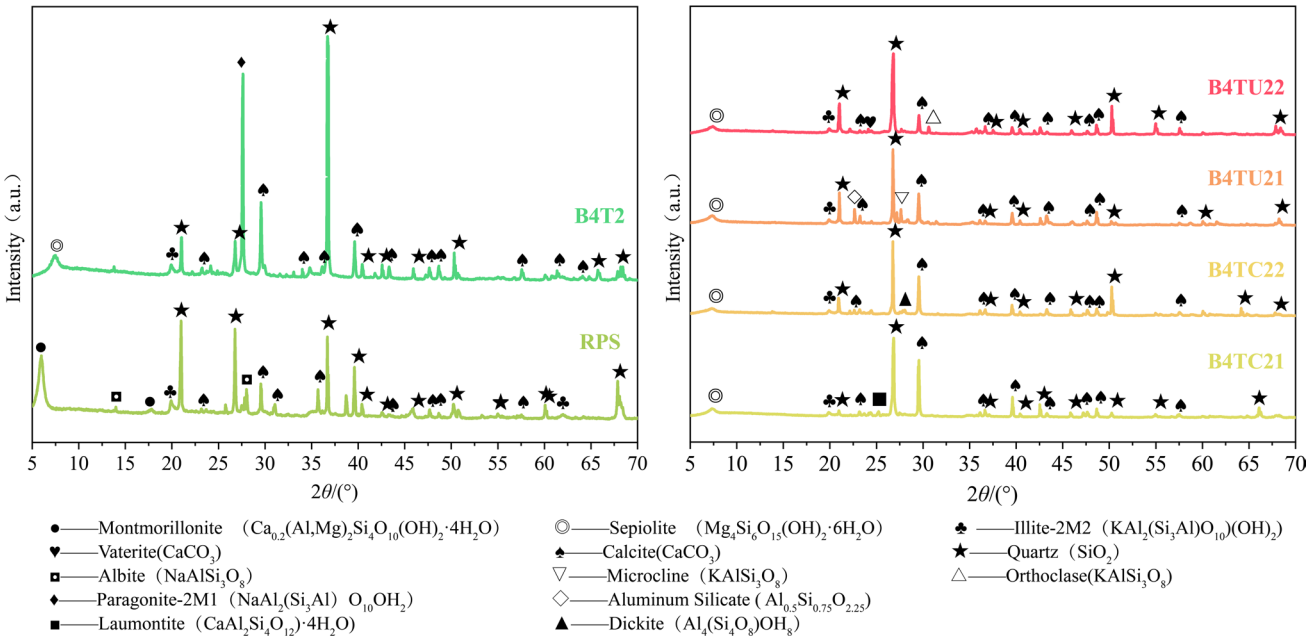

Fig. 7 XRD pattern of self-sorption biphasic injection method of cemented Pisha sandstone particles

crystal plane decreased, the sharpness weakened and broadened after the 10 mL$CaCl_2$ plus solvent treatment, and a new peak appeared simultaneously. Additionally, a new diffraction peak in the silica–aluminate phase with a broader base and weaker peak intensity appeared in the B4TU21 specimen, whereas the aragonite diffraction peak in the (110) crystal plane appeared in the B4TU22 specimen. The diffraction peaks of the B4TU22 specimen showed the corresponding diffraction peaks of aragonite at the (110) crystal plane; however, the intensity of the diffraction peaks was not high, indicating its low crystallization. In summary, some of the quartz in the Pisha sandstone undergoes dissolution in the complex environment of bacterial and cementing liquids, which provides silica–aluminate roots for the formation of silica–aluminate.

The XRD-pattern analysis comparison reveals that the calcite phase in the $CaCl_2$ – and CO(NH2)2-treated groups had diffraction peaks corresponding to the (104) (113) crystal plane but that as more additional solvent was injected, the peak sharpness gradually weakened, the peak intensity gradually decreased, and the degree of crystallization decreased. Additionally, it was found that the UCS of the calcium source treatment group increased from 226 to 331 kPa as the calcium carbonate yield increased, which indicated that the degree of calcite crystallization was not the only criterion to evaluate the good or bad cementation performance. This is primarily due to the calcium carbonate yield partially compensating for the deterioration caused by the decrease in crystallization to a certain extent; meanwhile, the calcium carbonate yield of the urea treatment group was higher than that of the test group injected with 10 mL $CaCl_2$ solvent. However, the calcite crystallization degree was not as good as that of the calcium source group, and the UCS value was lower than that of the calcium source group, which indicated that the calcium carbonate yield could not compensate for the degradation effect when the crystallization degree was too low.

The RPS was analyzed by the MDI JADE 9 software and the montmorillonite mineral diffraction peak appeared at ($2\theta = 6.0°$), which disappeared after the microbial curing treatment, with a new mineral diffraction peak appearing at ($2\theta = 7.3°$). This indicates that montmorillonite dissolution occurs, which is a very complex process including physical or chemical adsorption, ion exchange, molecular trapping, and chemical decomposition (Temuujin et al. 2006). The skeletal elements constituting the montmorillonite are divided into interlayer cations (Ca and Mg), basal (Si), and marginal surfaces (Mg and Al). From the perspective of the total dissolution of montmorillonite, the theoretical value of the order of dissolved substance concentration is Si > Al > Mg > Ca. The CO_3^{2-} brine-clay mineral solubility test measurement test shows that the concentration of the montmorillonite-dissolved substance is Mg > Ca > Si > Al. This is primarily due to the priority of the edge surface dissolution over the base surface dissolution, whereas the Ca^{2+} concentration is close to 2 mmol/kg (Jeon et al. 2018). Combined with the XRD analysis, although Al^{3+} dissolution from the edge face is preferred, Al^{3+} and Si^{4+} combined with precipitation to form a new mineral phase, so B4T2, B4TC21, and B4TU21 can be detected as the silica–aluminate phase

in the XRD. Meanwhile, Si^{4+} combined with Mg^{2+} to form a new clay mineral phase seafoam-type magnesium silicate ($2\theta = 7.3°$), which has no montmorillonite of ion exchange and swelling ability and has a strong adsorption capacity. Except for B4TC21, no new Ca-containing mineral phase was found, indicating that Ca^{2+} dissolved from endogenous calcium montmorillonite in the Pisha sandstone and reacted with CO_3^{2-} to form calcium carbonate.

Based on SEM microstructure cementation mechanism analysis

As shown in Fig. 8, the microscopic morphological characteristics of the top and bottom of the MICP-cured sand column under different applied solvents were observed using an SEM magnified 500 times. The top and bottom microstructures of the pure bacterial solution B4T2 are shown in Fig. 8a, d, where the top Pisha sandstone particles are wrapped by calcium carbonate precipitation. Furthermore, the mineralization products only play the role of wrapping, resulting in poor interfacial cementation of the particles. As shown in (Fig. 8d), the mineralization products increase the degree of wrapping of Pisha sandstone particles, and some large pores are sealed to increase the interparticle cementation force. Thus, the pure bacterial liquid test group B4T2 macroscopically appears to be poorly cured at the top and better cured at the bottom.

The microstructure of the top of B4TC22 in the calcium source treatment group is shown in (Fig. 8b). Following treatment with a low concentration of $CaCl_2$, the bacteria can adsorb uniformly on the surface of Pisha sandstone grains, and the agglomerated small crystal precipitates form a crystal cluster coating (calcium carbonate envelope), covering wrapping the surface of individual sand grains and bridging adjacent grains. At this time, the calcium carbonate deposits have a good connection effect and stability between the sand grains. Furthermore, microorganisms migrate through the pore channels and adsorb to the pore channels of the sand column because of percolation, inducing the formation of calcium carbonate precipitate when the colloidal fluid flows through the pore channels. Because the bacteria were used as nucleation sites at the beginning of the reaction, the calcium carbonate precipitate was mainly nucleated, and the size of calcium carbonate was small enough to seal the pores of larger size. The unblocked pores, however, allow the cementing

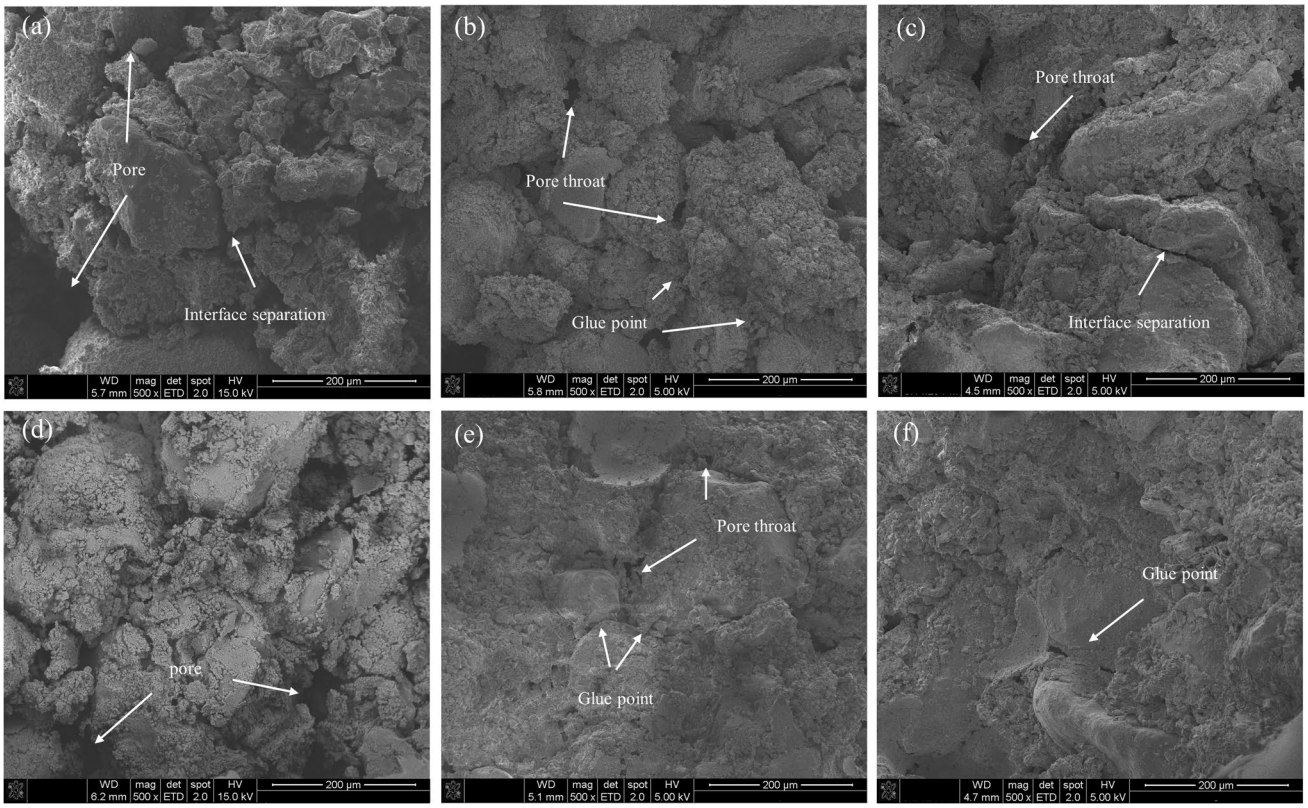

Fig. 8 SEM images of cemented Pisha sandstone particles (500×) under different applied solvents in the self-adsorption biphasic injection method. **a** Top microstructure of B4T2. **b** Top microstructure of B4TC22. **c** Top microstructure of B4TU22. **d** Bottom microstructure of B4T2. **e** Bottom microstructure of B4TC22. **f** Bottom microstructure of B4TU22

solution to enter the interior of the specimen and form new cementation sites, increasing the specimen's stability. As the reaction proceeds, the calcium carbonate crystals at the pore channel shown in (Fig. 8e) also increase and become larger, and the pore space decreases and closes gradually, forming cementation points and closely connecting multiple Pisha sandstone particles to form cemented bodies. Additionally, the compactness between particles is enhanced, thus making the sand body integral and gaining the ability to withstand external loads.

Figure 8c shows the microstructure of the top of B4TU22 in the urea-treated group. The top calcium carbonate agglomerates deposited on the surface of Pisha sandstone increase the particle size and fill the pore space. However, the calcium carbonate cementation layer appears separated from some particles, not completely cementing the Pisha sandstone particles, resulting in poor macroscopic mechanical properties. As shown in Fig. 8f, the natural infiltration treatment at the bottom caused the bacteria to adsorb more uniformly on the Pisha sandstone particles and pore channels, and the gaps between the Pisha sandstone particles were almost filled with crystals.

Comparing the results of the calcium source and urea treatment, it was found that the macroscopic mechanical properties of the urea-treated group still performed poorly. This was due to the presence of a large amount of CO_3^{2-} inside the specimen following the hydrolysis of urea during the resting process, as well as the formation of calcium carbonate precipitation when the cement flowed through the pore channel, with CO_3^{2-} and Ca^{2+} existing in the system in a supersaturated state. Furthermore, the calcium carbonate precipitate generated at this stage was not completely formed by microbial induction, at which time the calcium carbonate precipitates in a predominantly homogeneous nucleated form. The different nucleation methods of calcium carbonate combine to fill the pores and wrap the Pisha sandstone particles. Nevertheless, because the supersaturated precipitated calcium carbonate crystals have no cementation effect, the cementation effect of the microbial mineralization products is weakened. This results in the interface separation between the Pisha sandstone particles and the calcium carbonate inclusions, which macroscopically shows a high calcium carbonate yield but has little effect on the strength improvement. When combined with the thermodynamic theory of crystal nucleation, the formation of crystal nuclei is classified as homogeneous nucleation and heterogeneous nucleation. The calcium carbonate crystals in the calcium source injection group were mainly formed by heterogeneous nucleation with cementation, whereas the calcium carbonate crystals in the urea injection group were formed by both homogeneous and heterogeneous nucleation, resulting in the generated calcium carbonate having a poor cementation effect on the sand column.

Additionally, Fig. 8 shows that the cementation effect of calcium carbonate precipitation on the surface of Pisha sandstone particles can be divided into effective cementation and ineffective cementation, where ineffective cementation means that the calcium carbonate deposited on the surface of the particles only plays the role of wrapping and plays no role in cementing the adjacent particles. Effective cementation is mainly the effect of an effective cementation point. There are mainly two types of cementation point formation mode: (1) When the particles come into contact with the particles, bacteria adsorbed at the contact point and produce calcium carbonate crystals to form a cementation point, play a binding role. (2) Pisha sandstone particles are wrapped by calcium carbonate crystals, change their particle size, increase the roughness between particles, and cementation of adjacent particles, forming a contact cementation point. By contrast, it was found that the pore size inside the sand column was larger when treated with pure bacterial solution, and the calcium carbonate precipitation mainly wrapped the Pisha sandstone particles in the form of ineffective cementation. Furthermore, there were fewer effective cementation points between particles, which led to the inability to shape the specimens. The pore filling and cementation of particles were better after treatment with low concentration $CaCl_2$ solution, and its precipitated calcite could form effective cementation points and make the specimens more stable; $CO(NH_2)_2$ solution treatment effectively reduces the pore size and makes fewer pores between the particles. However, the interface between the calcium carbonate and the particles appears to separate, which forms ineffective cementation sites. Calcium carbonate is deposited on the surface of Pisha sandstone particles and forms cementation points, bridging adjacent particles to form agglomerates. Finally, the agglomerates continue to cement and merge, and this cementation network skeleton structure is the key to soil reinforcement. However, if the cementation point cementation is weak, forming ineffective cementation and only playing the role of filling and wrapping, it will result in an unstable skeleton structure and poor optimization of mechanical properties.

Discussion

Interaction between the mineralization products and Pisha sandstone grains

Figure 9 shows the microscopic mineralization morphology of microbially cured Pisha sandstone, treated with different additional solvents. It was found that microorganisms induced the formation of small calcium carbonate crystals, with a size ranging from 2 to 10 μm, and the small crystals interconnected and agglomerated to form a calcium carbonate crystal envelope. Figure 9a, b shows the morphological

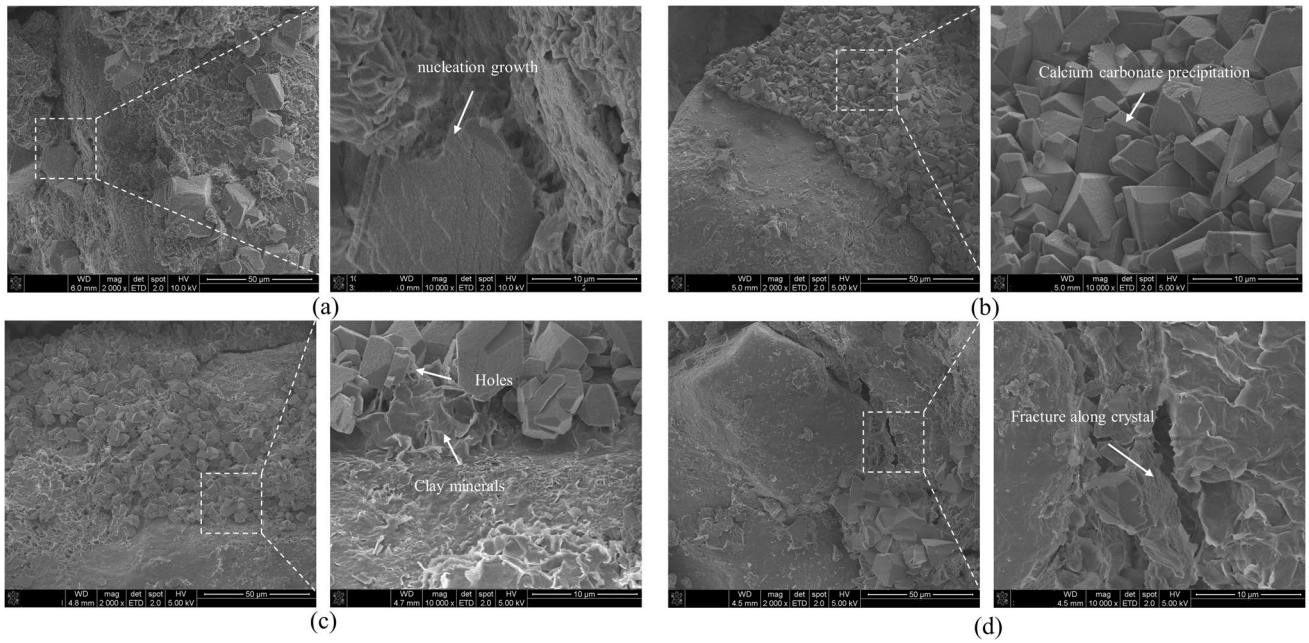

Fig. 9 SEM images of cementation curing mechanism (2000×, 10,000×) with different applied solvent treatments. **a** Top microstructure of B4TC22; **b** Top microstructure of B4TU22; **c** Bottom microstructure of B4TC22; **d** Bottom microstructure of B4TU22

structure of the microscopic mineralization of the calcium source treatment group B4TC22. The large crystals will use the small crystals that have formed as nucleation sites to form larger-sized calcium carbonate crystals after secondary nucleation (Fig. 9a). The Pisha sandstone's surface layer contains a layer of petal-like lamellar crystals (seafoam-type magnesium silicate) that act as an adhesive to the grains in phase with the irregular calcite crystals, preventing the microbially induced formation of calcium carbonate from being directly attached to the grains (Fig. 9b). This is attributed to bacterial adsorption onto montmorillonite in the Pisha sandstone, whereas mineral dissolution and crystal reprecipitation promote nucleation and growth of the crystal clusters. These results in calcium carbonate being deposited on the lamellar crystals that are mainly from the agglomeration effect following ion exchange reactions (Yuan et al. 2022).

Figure 9c, d shows the microscopic mineralization morphology structure of the urea-treated group B4TU22. As shown in Fig. 9c, the surface of the Pisha sandstone particles forms a layer of calcium carbonate crystal envelope, which has only a covering wrapping effect and does bridge the adjacent sand particles. This type of crystal precipitation is not sufficient to withstand high shear strength (Cheng et al. 2016a, b). Figure 9d shows that cracks appear between the crystals, which are formed because the large crystals are more cohesive, with the adjacent crystals weakly cemented. Additionally, the minerals separate along the crystal material and fracture along the crystal, leading to the low compressive strength of the urea-treated group, which also indicates that the calcium carbonate precipitates formed after the urea treatment are homogeneous and heterogeneous nucleated cemented bodies.

Comparing the results of the calcium source and urea treatment, it can be seen that the calcium carbonate formed by the MICP is attached to the surface of the Pisha sandstone particles in an irregular shape. However, the calcium carbonate precipitation in the calcium source treatment group is closely cemented to the Pisha sandstone particles, whereas the calcium carbonate precipitation in the urea treatment group has interfacial media and cluster fractures with the Pisha sandstone. Thus, the macroscopic performance of the calcium source treatment is superior.

Regulatory role of bio-organic matter

Additionally, the holes found in the calcium carbonate crystals in Fig. 9, which were left by bacterial dissolution, suggest that there are traces of bacterial activity in $CaCO_3$. FTIR was used to effectively identify the functional groups in the mineralized products. The FTIR spectra of the biomineralized products produced by different applied solvent treatments are shown in Fig. 10, and the chemical structure functional groups of the characteristic bands of the mineralized products are listed in Table 3. A comparison of the characteristic FTIR bands revealed that the Si–O stretching vibration absorption peak appeared at 778 cm^{-1}, and when the additional solvent was added, the sharp absorption peak

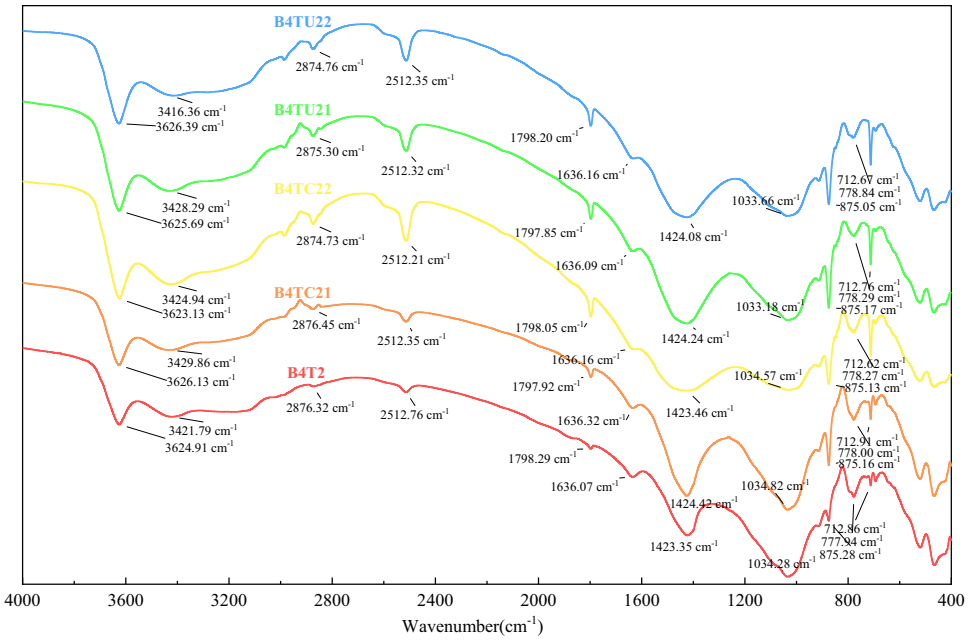

Fig. 10 FT-IR mapping of mineralization products under different treatments

Table 3 Infrared vibrational bands of EPS products

Band (cm^{-1})	Functional group	Possible compounds
3626–3416	O–H and N–C stretching	Carbohydrates, proteins, lipids
2876–2874	C–H stretching	Proteins, lipids
1798–1797	C = O stretching	Fatty esters or carboxylic acid (lipids)
1636	N–H and C–N stretching	Proteins, N-acetylated amino sugars
1034–1033	C–O stretching	Polysaccharide

changed to a broad peak with a slight arc, indicating a partial dissolution of the Si–O functional group. Additionally, vibrational absorption peaks were observed at 712, 875, and 1424 cm^{-1}, which are close to the published values (Wang et al. 2022; Qian et al. 2021a, b), caused by stretching vibrations of the C–O bonds of calcium carbonate in the mineralized product. By comparing the injection of pure bacterial solution and the experimental group with the additional solvent, it was found that the absorption peak at 1424 cm^{-1} changed from being sharp to having an absorption peak with an arc after the injection of the additional solvent. Additionally, the tiny vibrations near 712 and 875 cm^{-1} became sharper, indicating that the addition of the additional solvent increased the degree of ordering of the microbially induced calcium carbonate structure in the system.

Meanwhile, O–H and N–C bond stretching vibrations of carbohydrates, proteins, and lipids were detected at 3626–3416 cm^{-1}; C–H bond stretching vibrations of proteins, and lipids were detected at 2876–2874 cm^{-1}; C = O stretching vibrations of fatty esters or carboxylic acids (lipids) were detected at 1798–1797 cm^{-1}. N–H bond and C–N bond stretching of proteins and N-acetylated amino sugars were detected at wave number 1636 cm^{-1}. Polysaccharide C–O stretching vibrations were detected at 1034–1033 cm^{-1}, indicating that bacteria secrete extracellular polymers and participate in the MICP reaction. Bacteria also provide templates for the MICP crystal nucleation through metabolism and become heterogeneous nucleation sites for mineral deposition during the reaction, which promotes calcium carbonate precipitation but changes crystal growth morphology. Therefore, MICP nuclei are mainly formed by non-homogeneous nucleation, which is also the reason for the formation of irregular crystal morphology of biomineralization products.

Mineralization product crystals contain functional groups such as carboxyl, hydroxyl, and phosphate, which have been reported by many scholars (Zhang et al. 2020; Wang and Liu 2021). These charged groups collaborate with the bacteria and EPS during the crystal nucleation process. The nucleation process begins with the attraction system combining bacteria and calcium ions to form active sites. The negatively charged functional groups in the EPS act on the bacterial cell wall to enhance the electrostatic attraction on the bacterial surface. Furthermore, calcium ions accumulate on the surface of the cell wall. Simultaneously, urease decomposes urea in solution to produce carbonate ions, which

promote the production of an amorphous calcium carbonate precipitation. Finally, phase changes to form calcite with thermodynamic stability.

Bacterial autolysis and EPS contain carboxyl and hydroxyl groups that can act as heterogeneous nuclear sites, reducing the energy needed for precipitation and increasing the precipitation rate. However, besides the effect of microbial action on biomineralization products, the effect of the mineral composition of the Pisha sandstone cannot be ignored. Furthermore, montmorillonite solubilization produces free magnesium ions, which can inhibit calcite growth and promote amorphous calcium carbonate phase change to form aragonite. Combined with the XRD analysis, it is clear that the degree of crystallization of the biomineralization products varies, and the effect of magnesium ions on reducing calcite crystallization is more pronounced after urea treatment. This may be due to the different promotion of mineralization caused by the type of additional solution and the amount of injection.

Conclusion

MICP based on urea hydrolysis is one of the most important techniques for stabilizing soils because it can improve the mechanical properties of soils. This paper discusses the application of the traditional single-phase injection method and self-absorption two-phase injection method on microbially cured Pisha sandstone and analyzes the advantages of the self-absorption two-phase injection method by adding an added solvent to improve the distribution of bacteria in the sand column. The main conclusions of this paper are summarized as follows: (1) The specimens treated with unidirectional grouting, all exhibited better curing of one side sidewall, and the $CaCl_2$-treated and $CO(NH_2)_2$-treated groups showed decreased calcium carbonate production, decreased minimum curing depth, and curing volume with increasing additional solvent injection. By contrast, the cured specimens with two-way grouting were denser and more homogeneous, with the low concentration $CaCl_2$ treatment group showing an increase in calcium carbonate yield and a significant increase in the UCS with increasing additional solvent injection. However, the results for the $CO(NH_2)_2$ treatment group showed that 10 and 20 mL of urea injection had no significant effect on the increase in calcium carbonate yield. (2) The XRD analysis revealed that the calcite phase diffraction peaks corresponding to the $CaCl_2$-treated group and the $CO(NH_2)_2$-treated group at the (104) (113) crystal plane gradually weakened in peak sharpness and decreased in peak intensity with the increase of additional solvent injection. Furthermore, the degree of crystallization decreased, but the increase in calcium carbonate yield could compensate to some extent for the deteriorating effect of the reduced degree of crystallization on the overall properties of the specimens. In the environment of the bacterial liquid–collodion solution, montmorillonite undergoes dissolution, eliminating the characteristics of Pisha sandstone swelling in water. The Pisha sandstone particles are agglomerated to form agglomerates under the improvement of biomineralization, which effectively improves the stability of the Pisha sandstone soil body. (3) The SEM analysis showed that calcium carbonate is deposited on the surface of the Pisha sandstone particles and forms cementation points, bridging adjacent particles to form agglomerates. Calcium carbonate crystals in the calcium source injection group are mainly formed by heterogeneous nucleation with cementation. Additionally, the agglomerates continuously cement and merge to form the cementation network skeleton structure of the reinforced soil. By contrast, the calcium carbonate crystals in the urea injection group are formed by both homogeneous nucleation and heterogeneous nucleation, and the generated calcium carbonate has a poor cementation effect on the sand column, resulting in an unstable skeleton structure. Simultaneously, microscopic morphology with fracture along the crystal results in poor macroscopic mechanical properties. (4) Microbially induced calcite precipitation can achieve the curing of loose Pisha sandstone, but improving the curing effect is closely related to the curing conditions and needs to be considered from various aspects.

Acknowledgements We are very grateful to the College of Water Resources and Civil Engineering of Inner Mongolia Agricultural University for providing us with the experimental platform.

Author contribution Zhuojun Feng participated in the study design, experimental organization, and data analysis; Xiaoli Li participated in the manuscript review and revision; Xinhang Shao and Liming Wang made important suggestions.

Funding This work was supported by the National Natural Science Foundation of China (42067017).

Data availability All data generated or used in the study appear in the article. The data and materials obtained are authentic and valid. The data used to support the results of this study are available from the corresponding author.

Declarations

Ethics approval and consent to participate Not applicable.

Consent for publication Not applicable.

Competing interests The authors declare no competing interests.

References

Atashgahi S, Tabarsa A, Shahryari A, Hosseini SS (2020) Effect of carbonate precipitating bacteria on strength and hydraulic

characteristics of loess soil. Bull Eng Geol Env 79(9):4749–4763. https://doi.org/10.1007/s10064-020-01857-0

Cheng J, Han JC, Wang HY, Zhang Y, Zhang WH, Chen KH (2016a) Study on sand-fixing mechanism by feldspathic sandstone in Mu Us Sand Land. Journal of Soil and Water Conservation (5): 124–127. https://doi.org/10.13870/j.cnki.stbcxb.2016a.05.021.

Cheng L, Shahin MA, Mujah D (2016b) Influence of key environmental conditions on microbially induced cementation for soil stabilization. J Geotech Geoenviron Eng 143(1):1–11. https://doi.org/10.1061/(ASCE)GT.1943-5606.0001586

Cheng XH, Ma Q, Yang Z, Zhang ZC, Li M (2013) Dynamic response of liquefiable sand foundation improved by bio-grouting. J Geotech Eng 08:1486–1495

Cui MJ, Zheng JJ, Lai HJ (2017) Effect of method of biological injection on dynamic behavior for bio-cemented sand. Geotech Mech 38(11): 3173–3178. https://doi.org/10.16285/j.rsm.2017.11.012.

Geng K, Li X (2022) Performance analysis of sulfate Pisha-sandstone cement soil based on the grey entropy theory. KSCE J Civ Eng 26:584–595. https://doi.org/10.1007/s12205-021-0417-y

Geng K, Chai J, Qin Y, Li XL, Zhou H (2022) Collapse inhibition mechanism analysis and durability properties of cement-stabilized Pisha sandstone. Bull Eng Geol Environ 81:144. https://doi.org/10.1007/s10064-022-02642-x

Gong Y (2022) Study on air pollutant and CO_2 emission inventory and abatement costs in China's cement industry. Zhejiang University

Hoang T, Alleman J, Cetin B, Ikuma K, Choi S-C (2018) Sand and silty-sand soil stabilization using bacterial enzyme–induced calcite precipitation (BEICP). Can Geotech J 56(6):808–822. https://doi.org/10.1139/cgj-2018-0191

Jeon PR, Kim D-K, Lee C-H (2018) Dissolution and reaction in a CO_2-brine-clay mineral particle system under geological CO_2 sequestration from subcritical to supercritical conditions. Chem Eng J 347:1–11. https://doi.org/10.1016/j.cej.2018.04.052

Li H, Tang CS, Yin LY, Liu B, Lu C, Wang DL, Pan XH, Wang HL, Shi B (2021a) Experimental study on surface erosion resistances and mechanical behavior of MICP-FR-treated calcareous sand. Geot Eng 43(10):1941–1949.https://doi.org/10.11779/CJGE2021a10021

Li XL, Zhao XZ, Shen XD (2021b) Influence mechanism of alkali excitation on strength and microstructure of Pisha sandstone geopolymer cement composite soil. Trans Chin Soc Agric Eng 37(12): 73–81. https://doi.org/10.11975/j.issn.1002-6819.2021b.12.009.

Liang ZS, Wu ZR, Yao WY, Noori M, Yang CQ, Xiao PQ, Leng YB, Deng L (2019) Pisha sandstone: causes, processes and erosion options for its control and prospects. Int Soil Water Conserv Res 7(1):1–8. https://doi.org/10.1016/j.iswcr.2018.11.001

Liu X, Shen XD, Xue HJ, Liu Q, Geng KQ (2020) Grey entropy analysis of strength and pore structure evolution of cement-solidified Pisha sandstone. Trans Chin Soc Agric Eng 36(24): 125–133. https://doi.org/10.11975/j.issn.1002-6819.2020.24.015.

Qabany A, Soga K (2013) Effect of chemical treatment used in MICP on engineering properties of cemented soils. J Géotechnique 63(4):331–339. https://doi.org/10.1680/geot.SIP13.P.022

Qian CX, Ren XW, Rui YF, Wang K (2021a) Characteristics of bio-CaCO3 from microbial bio-mineralization with different bacteria species. Biochem Eng J 176:1–10. https://doi.org/10.1016/j.bej.2021.108180

Qian CX, Rui YF, Wang CY, Wang XM, Xue B, Yi HH (2021b) Bio-mineralization induced by Bacillus mucilaginosus in crack mouth and pore solution of cement-based materials. Mater Sci Eng, C 126:1–11. https://doi.org/10.1016/j.msec.2021.112120

Rowshanbakht K, Khamehchiyan M, Sajedi EH, Nikudel MR (2016) Effect of injected bacterial suspension volume and relative density on carbonate precipitation resulting from microbial treatment. Ecol Eng 89:49–55. https://doi.org/10.1016/j.ecoleng.2016.01.010

Temuujin, J, Senna M, Jadambaa T, Burmaa D, Erdenechimeg S, Kenneth S MacKenzie KJ (2006) Characterization and bleaching properties of acid-leached montmorillonite. J Chem Technol Biotechnol 81(4). https://doi.org/10.1002/jctb.1469.

Tian ZF, Tang XW, Li J, Xiu J, Xue ZJ (2021) Influence of the grouting parameters on microbially induced carbonate precipitation for soil stabilization. Rock and Soil Mechanics 38(9):755–767. https://doi.org/10.1080/01490451.2021.1946623

Wang L, Liu SH (2021) Mechanism of sand cementation with an efficient method of microbial-induced calcite precipitation. Materials 14(19):5631. https://doi.org/10.3390/ma14195631

Wang T, Yang YJ, Deng L, He LY, Xu MW, Yang CQ, Liang ZS (2020) Effects of different solid microbial agents on soil properties of Pisha sandstone and the growth of alfalfa. Trans Chin Soc Agric Eng 36(8): 96–102. https://doi.org/10.11975/j.issn.1002-6819.2020.08.012.

Wang Z, Zhang J, Li M, Guo S, Zhang J, Zhu G (2022) Experimental study of microorganism-induced calcium carbonate precipitation to solidify coal gangue as backfill materials: mechanical properties and microstructure. Environ Sci Pollut Res Int. https://doi.org/10.1007/s11356-022-18975-9

WhIffin VS (2004) Microbial $CaCO_3$ precipitation for the Production of biocement. Murdoch University, Perth, Australia

Yang J, Li XL, Wang H, Geng KQ (2021a) A study of the structural evolution and strength damage mechanisms of Pisha-sandstone cement soil modified with Fly Ash. J Renew Mater 9(12):2241–2260. https://doi.org/10.32604/jrm.2021.015565.

Yang X, Wang Y, Wang S Evans TM, Stuedlein AM, Chu J, Zhao C, Liu HL (2021b) Homogeneity and mechanical behaviors of sands improved by a temperature-controlled one-phase MICP method. Acta Geotech 6:1417–1427. https://doi.org/10.1007/s11440-020-01122-4

Yang ZQ, Qin FC, Li L, Ren XT, Qian QY, Han J (2019) Spatial distribution characteristics of soil organic matter and its influencing factors in small watershed of feldspathic sandstone region. Trans Chin Soc Agric Eng 35(17): 154–161. https://doi.org/10.11975/j.issn.1002-6819.2019.17.019.

Yao WY, Xiao PQ, Wang YC, Shen ZZ (2019) Advances in erosion management technology in Pisha sandstone area. .Advances in water conservancy and hydropower science and technology 39(05):1–9+15. https://doi.org/10.3880/j.issn.1006-7647.2019.05.001.

Yin LY, Tang CS, Xie YH, Lu C, Jiang LJ, Shi B (2019) Factors affecting improvement in engineering properties of geomaterials by microbial-induced calcite precipitation. Rock and Soil Mechanics (07): 2525–2546. https://doi.org/10.16285/j.rsm.2018.0520.

Yu XN, Qian CX, Sun LZ (2018) The influence of the number of injections of bio-composite cement on the properties of bio-sandstone cemented by bio-composite cement. Construction and Building Materials 164(MAR.10): 682–687. https://doi.org/10.1016/j.conbuildmat.2018.01.014.

Yuan H, Liu K, Zhang CG (2022) Zhao ZL (2022) Mechanical properties of Na-montmorillonite-modified EICP-treated silty sand. Environ Sci Pollut Res Int 29(7):10332–10344. https://doi.org/10.1007/s11356-021-16442-5

Zhang CH, Li XL, Jyu JJ, Li FC (2020) Comparison of carbonate precipitation induced by Curvibacter sp. HJ-1 and Arthrobacter sp. MF-2: Further insight into the biomineralization process. J Struct Biol 212(2):1–9. https://doi.org/10.1016/j.jsb.2020.107609.

Zhang P, Yao WY, Liu GB, Xiao PQ (2019a) Research progress and prospects of complex soil erosion. Transactions of the Chinese Society of Agricultural Engineering (Transactions of the CSAE) 2019a, 35(24): 154–161. https://doi.org/10.11975/j.issn.1002-6819.2019a.24.019.

Zhang Q, Song ZP, Li XL, Wang JB, Liu LJ (2019b) Deformation behaviors and meso-structure characteristics variation of the

weathered soil of Pisha sandstone caused by freezing-thawing effect. Cold Regions Science and Technology 167(C): 1–17. https://doi.org/10.1016/j.coldregions.2019b.102864.

Zhao Q (2014) Experimental study on microbially induced calcium carbonate precipitation (MICP) cured soil. China University of Geosciences, Beijing

Zhao XZ, Li XL, Shen XD, Yang J (2021) Dynamic mechanical properties of Pisha sandstone geopolymer cement composite soil using SHPB. Transactions of the Chinese Society of Agricultural Engineering 37(17): 310–316. https://doi.org/10.11975/j.issn.1002-6819.2021.17.036.

Zhu JH, Li XL (2022) Strength and microscopic mechanism analysis of CFBCA-based geopolymer–Pisha sandstone cement composite soil. Environ Sci Pollut Res: 1-14.https://doi.org/10.1007/s11356-022-20427-3